

UNIFIED ORBIT FEEDBACK AT NSLS-II*

Y. Hidaka[†], G. M. Wang, Y. Tian, R. Smith, Y. Li, X. Yang
Brookhaven National Laboratory, Upton, NY, USA

Abstract

We have developed an orbit correction / feedback program to unify the existing orbit-related feedback systems for stable beam operation at NSLS-II. Until recently only a handful of beamlines have been benefiting from long-term orbit stability provided by a local bump agent program. To expand this to all the beamlines as well as correct more frequently, a new slow orbit feedback program called unified orbit feedback (UOFB) was written from scratch that works with the fast orbit feedback transparently, while accumulated fast corrector strength is continuously shifted to the slow correctors and RF frequency is adjusted for circumference change. UOFB can lock 3 different types of local bumps to the target offsets/angles for days: those for insertion device (ID) sources with only ID RF beam position monitors (BPM) or mixtures of ID RF BPMs and X-ray BPMs, and those for bending magnet sources with arc BPMs between which orbit correctors, dipoles and quadrupoles exist. Furthermore, this feedback can accommodate beamline user requests to enable/disable the feedback loop for their beamline and to change bump target setpoints without turning off the loop.

INTRODUCTION

The most critical stability requirement for beamline users at a third-generation light source like National Synchrotron Light Source II (NSLS-II) [1] is beam orbit stability at the source points. Some beamlines require the long-term beam angle stability to be 100-10 nrad at samples [2]. An active beamline components feedback [3] can substantially help, but it requires raw electron beam (e-beam) orbit stability to be at least on the order of a few hundred nrad.

To satisfy the requirements for the most sensitive beamlines, the first local bump agent (LBA) was successfully commissioned and put into operation in 06/2018 [4]. The program has been expanded to 5 beamlines since then. However, further expansion to all was difficult due to 1) conflicts with adjacent agents, 2) accumulating fast corrector strengths, and 3) incompatibility of bending magnet bump agents and the RF frequency feedback (RFFB).

To solve all these issues, we have recently implemented UOFB whose goal is to unify the slow orbit feedback (SOFB), fast orbit feedback (FOFB) and RFFB with the ability to offload accumulated fast corrector strengths to slow correctors and the flexibility to adjust all types of local bumps at any time.

UNIFYING ORBIT FEEDBACKS

The main algorithm implemented in the Python script for UOFB to suppress the long-term orbit drift is the SOFB

* Work supported by U.S. DOE under Contract No. DE-SC0012704.

[†] yhidaka@bnl.gov

component of UOFB and is based on the following equations [5]:

$$\Delta\vec{I}_{\text{SOFB}} = \Delta\vec{I}_{1,\text{SOFB}} + \Delta\vec{I}_{2,\text{SOFB}}, \quad (1)$$

$$\Delta\vec{I}_{1,\text{SOFB}} = R_{\text{SOFB}}^{-1} \cdot \Delta\vec{U}, \quad (2)$$

$$\Delta\vec{I}_{2,\text{SOFB}} = R_{\text{SOFB}}^{-1} \cdot (R_{\text{FOFB}} \cdot \Delta\vec{I}_{\text{FOFB}}), \quad (3)$$

where $\Delta\vec{U}$ is the measured orbit error and $\Delta\vec{I}_{\text{SOFB}}$ is the final slow corrector setpoint change vector, which is the sum of $\Delta\vec{I}_{1,\text{SOFB}}$ (changes that would be applied to correct $\Delta\vec{U}$ when FOFB is not running) and $\Delta\vec{I}_{2,\text{SOFB}}$ (changes that will shift the DC part of fast corrector currents $\Delta\vec{I}_{\text{FOFB}}$ to slow corrector currents). The inverted (usually via singular value decomposition) orbit response matrix (ORM) for the slow correctors is denoted by R_{SOFB}^{-1} , while R_{FOFB} is the ORM for the fast correctors. Finally, to make the application of $\Delta\vec{I}_{\text{SOFB}}$ transparent to FOFB, we must modify the reference orbit of FOFB by $\Delta\vec{W}$ to match the predicted orbit movement [5]:

$$\Delta\vec{W} = R_{\text{SOFB}} \cdot \Delta\vec{I}_{1,\text{SOFB}}. \quad (4)$$

UOFB also includes the functionality of RFFB to compensate the long-term circumference change ΔC with an RF frequency adjustment. Since some of the slow correctors are in the dispersive sections at NSLS-II, the energy change δ induced by ΔC would be absorbed into $\Delta\vec{I}_{\text{SOFB}}$ if we simply use R_{SOFB} as is. To avoid this, we replace Eqs. (2) and (3) with the following:

$$\Delta\vec{I}_{1,\text{SOFB}} = \mathcal{N} \cdot \Delta\vec{\phi}_{1,\text{SOFB}}, \quad (5)$$

$$\Delta\vec{I}_{2,\text{SOFB}} = \mathcal{N} \cdot \Delta\vec{\phi}_{2,\text{SOFB}}, \quad (6)$$

where \mathcal{N} is the null space of the energy response matrix D for $\Delta\vec{I}_{\text{SOFB}}$ such that $D \cdot (\mathcal{N} \cdot \Delta\vec{\phi}) = 0$, i.e., preserving beam energy. The $\Delta\vec{\phi}$ vectors and energy changes can be obtained by solving

$$\begin{bmatrix} \Delta\vec{\phi}_{1,\text{SOFB}} \\ \delta_1/w \end{bmatrix} = Q^{-1} \cdot \Delta U, \quad (7)$$

$$\begin{bmatrix} \Delta\vec{\phi}_{2,\text{SOFB}} \\ \delta_2/w \end{bmatrix} = Q^{-1} \cdot (R_{\text{FOFB}} \cdot \Delta\vec{I}_{\text{FOFB}}), \quad (8)$$

where the total energy compensation needed by the frequency change is given by $\delta = \delta_1 + \delta_2$. The matrix Q is defined as

$$Q = [R_{\text{SOFB}} \cdot \mathcal{N} \quad w\vec{\eta}], \quad (9)$$

with $\vec{\eta}$ and w being the dispersion function and a scaling factor (10 for the NSLS-II storage ring), respectively.

LOCAL BUMPS

UOFB allows correction of local bump offsets and angles. There are 3 types of local bumps at NSLS-II. The first and most prevalent and simplest type is the ID RF-BPM bump. A user has a choice to specify an offset and an angle for a straight populated with IDs. This pair of setpoint values can be readily converted to the target position values

for the 2 ID RF BPMs bounding an ID since there are no correctors or quadrupoles between them. Technically, there are orbit correctors controlled by orbit feedforward systems to cancel the residual field integrals of IDs between the BPMs. As long as the feedforward tables are up to date, the effect of these dedicated correctors can be ignored.

The second bump type is for bending magnets (BMs). Unlike ID RF bumps, there are multiple orbit correctors and quadrupoles between the BPMs bounding a BM. The formula to estimate the offset and angle at the source extraction point within the BM were derived, taking into account the current corrector kick angles and quadrupole strengths [6]. As the values of these magnet properties are not exactly known (due to calibration inaccuracy, hysteresis, and relative quadrupole center deviation), the BM offset and angle estimates are not as reliable as those for the ID RF bumps. BM bumps are also susceptible to the beam energy fluctuation as one of the BPM pair used to compute the offset/angle is dispersive. Nonetheless, they still work for the purpose of roughly maintaining the source position and angle for BMs.

The last type is an ID bump with an RF BPM and an X-ray BPM (X-BPM). This bump will be referred to as an X-BPM bump for simplicity. The beamlines (“X beamlines” for short) at Cells 3 (C03), 16 (C16), and 17 (C17) are equipped with front-end X-BPMs [7]. These BPMs are located approximately 15 m downstream from the electron beam source, and hence, give us very accurate angle estimates. For this type of bump, the absolute positions for the RF BPM and X-BPM are specified as targets. Since the X-BPM reading becomes unreliable because of less photons reaching the X-BPM when the ID gap is opened, the switch for the X-BPM bump is automatically disabled once the gap goes above a certain threshold. Similarly, the feedback is also disengaged if the gap changes by more than 150 μm from the gap value when the feedback was started.

For the X beamlines, both an ID RF bump and ID X-BPM bump are available, but only one type can be selected at any moment. Though X-BPM bumps are used during beamline experiments for the best orbit stability, RF bumps are still required to handle the situations where the ID gaps must be open, thereby rendering X-BPM bumps unusable.

The base ORM used for the SOFB component is the 360-by-360 ideal matrix computed by ELEGANT [8]. There are 180 horizontal and 180 vertical arc BPMs as well as 180 horizontal and vertical slow correctors. (If a measured ORM is used, some singular values must be cut to avoid excessive sensitivity to orbit noise, but at the cost of elevated residual orbit errors.) Then R_{SOFB} is modified by replacing some rows with the responses of RF BPM positions for ID RF bumps, offsets/angles for BM bumps, and X-BPM positions (i.e., angle response of e-beam orbit multiplied by the drift space of 15 m) for ID X-BPM bumps.

UOFB has been implemented such that the target value of the bump for a beamline can be adjusted without disabling the global feedback switch or the local beamline feedback switch. The only exception is when a user at the X beamlines wants to switch from the ID RF bump to the X-BPM bump, or vice versa. In this case, the local

beamline switch must be disabled first before the bump type selection can be changed. As additional orbit stability safety, the feedback also checks whether a requested bump change is too large and rejects such a request if so determined.

All beamlines except for the X beamlines are always enabled and have no ability to disable their local feedback switches. Users at the X beamlines are given the control to re-enable their local switches because of the automatic disengagement mechanism. Furthermore, C17 users are given a special permission to alter their bump setpoint without calling Control Room (CR) due to their unique environment (i.e., vulnerable to thermal floor motion caused by a vehicle tunnel underneath) that necessitates relatively frequent bump adjustments. Note that all beamlines can request bump adjustments via CR at any time.

During the UOFB test week, too large X-BPM reading spikes up to 10 μm at C03 were observed. These sudden jumps are transient in nature and occur because the slow corrector changes are not as fast as FOFB orbit reference change and that ramping of all the slow correctors are not synchronized. This forced us to reduce the correction percentage for each iteration from 70% to 10%, to keep such spikes under 1-2 μm . Obviously, this diminished the feedback ability to quickly correct orbit error or bump changes. An effort is ongoing to suppress these transient spikes without relying on the gain reduction by instead tweaking the FOFB configuration. However, as a temporary measure, the feature called “Accelerated Correction Mode” was implemented. Whenever a large correction is needed, the feedback goes into this mode in which the correction frequency is increased from the nominal 5 s to 2 s with 20% correction until required correction becomes small enough.

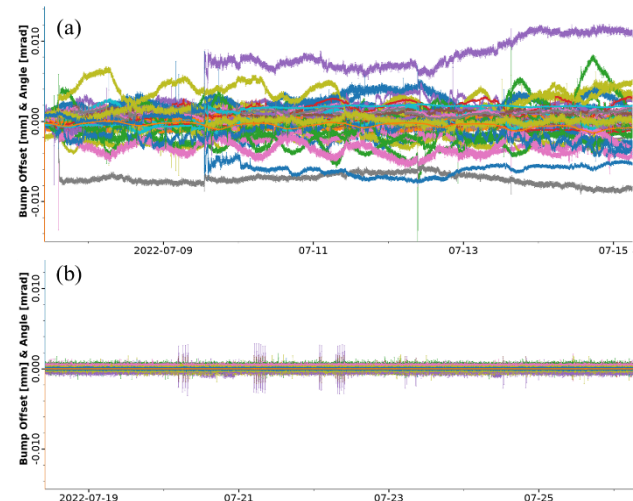


Figure 1: Local bump offset/angle changes for ID beamlines without X-ray BPMs during (a) LBA and (b) UOFB weeks.

DEPLOYMENT INTO OPERATION

Upon receiving only positive or neutral feedback comments from beamline users after the test week, UOFB was officially deployed for beamline operation on 7/18/2022 at NSLS-II. In this section, one week (7/7-7/15/2022) of

operation in the existing orbit feedback mode (FOFB + Local Bump Agents), the LBA week for short, is compared against one week (7/18-7/26/2022) with UOFB. There was no beam dump in both weeks. During the UOFB week, the global switch was briefly turned off between 14:56 and 15:07 on 7/20 for an experiment with beamline users.

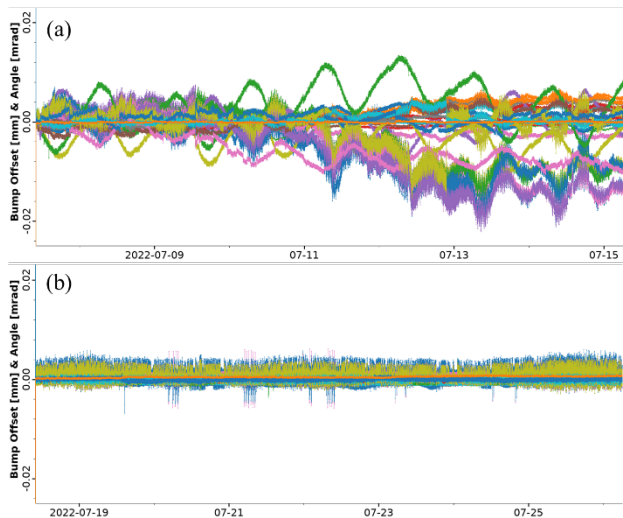


Figure 2: Local bump offset/angle changes for BM beamlines during (a) LBA and (b) UOFB weeks.

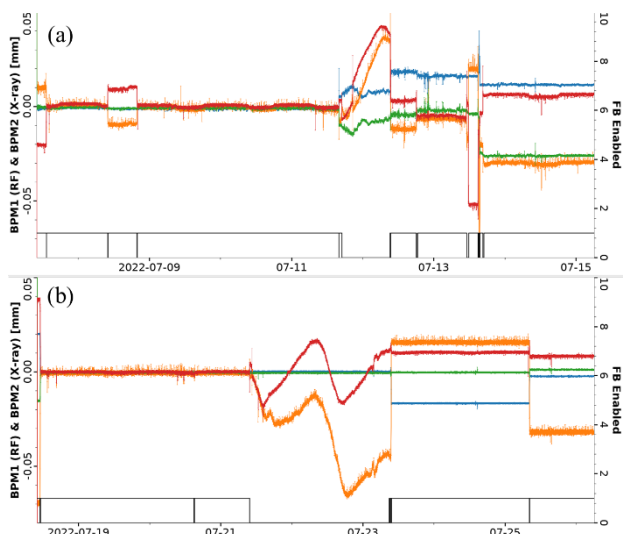


Figure 3: Local bump RF and X-BPM position changes for C17 during (a) LBA and (b) UOFB weeks. Feedback states (0=Off, 1=On) shown by “FB Enabled” (black lines).

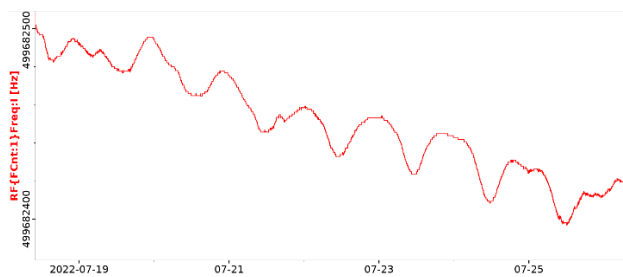


Figure 4: RF frequency history during the UOFB week.

Figure 1 compares the local bump offset and angle read-back changes in both planes for the ID beamlines without

X-BPMs. In the LBA week only 2 beamlines were feed-backed, while all 13 beamlines in this category were corrected in the UOFB week. Beamline users did not request any bump setpoint adjustments, except for the C19 horizontal angle bump (grey line in Fig. 1a) near the beginning of the LBA week.

As shown in Fig. 2, none of the BM bumps were feed-backed in the LBA week, while all 9 operational BM bumps were included in UOFB (though the data for one BM were not being archived, and hence not shown).

The X beamlines were not expected to see much improvement, as all of them were already feed-backed with LBA. Nonetheless, as Fig. 3 shows, the stability with UOFB appears slightly better probably due to more frequent corrections. In both weeks, there were long periods of the feedback being off where the black lines “FB Enabled” go to zero. The large drifts in these intervals illustrate the inability of FOFB alone to maintain the bump angle to a sufficient precision desired by beamline users. C17 users made bump adjustments several times, shown as steps, during both weeks.

The RFFB component of UOFB properly worked as shown in Fig. 4. Figure 5 demonstrates the fast-to-slow corrector shifting capability (the vertical data not shown due to space limit). The occasional downward spikes extending outside of the plot region are not real, caused by glitches in the readback.

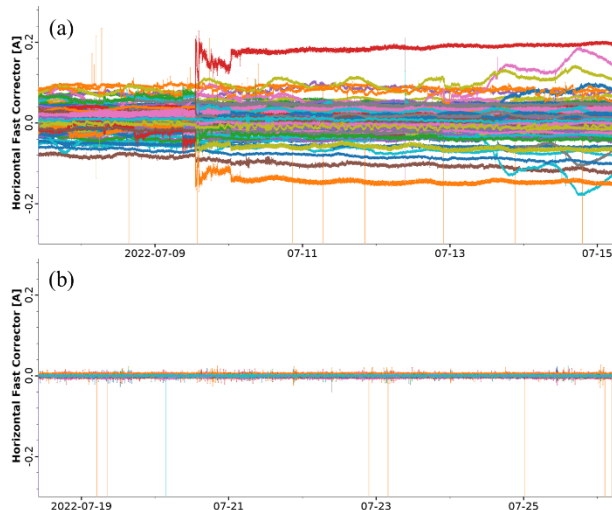


Figure 5: Horizontal fast corrector history during (a) LBA and (b) UOFB weeks.

CONCLUSION

A new orbit feedback called UOFB was implemented to provide excellent long-term orbit stability for all the existing beamlines at NSLS-II. The new system has been successfully tested and officially deployed into beamline operation recently. In addition to the source stability, UOFB compensates circumference change by adjusting the ring RF frequency as well as continuously distributes accumulated fast corrector kicks into slow correctors. This program can also accommodate 3 different types of local bumps and perform flexible adjustments when on-demand requests are received from beamline users.

REFERENCES

- [1] G. M. Wang, T. Shaftan, F. Willeke, *et al.*, “NSLS-II SR Commissioning Report”, BNL Technical Note, NSLSII-ASD-TN-168, 2015.
- [2] G. M. Wang, “Advances in Beam Stability in Low-Emittance Synchrotron Light Sources”, in *Proc. IPAC'21*, Campinas, Brazil, May 2021, paper FRXA02.
- [3] P. Ilinski, “Active beamline feedback implementation for photon beam stability”, 7th DLSR Workshop (2021).
- [4] Y. Hidaka *et al.*, “Improvements in Long-Term Orbit Stability at NSLS-II”, in *Proc. IPAC'19*, Melbourne, Australia, May 2019, pp. 4070-4073. doi:10.18429/JACoW-IPAC2019-THPRB104
- [5] N. Hubert, L. Cassinari, J. Denard, A. Nadji, and L. S. Nadolski, “Global Fast Orbit Feedback System Down to DC using Fast and Slow Correctors”, in *Proc. DIPAC'09*, Basel, Switzerland, May 2009, paper MOOC01, pp. 27-31.
- [6] Y. Hidaka, Y. Hu, B. Podobedov, R. Smith, Y. Tian, and G. Wang, “Fast-Orbit-Feedback-Compatible ID Local Bumps with RF and X-ray BPMs at NSLS-II”, BNL Technical Note, NSLSII-ASD-TN-353, 2021.
- [7] P. Ilinski, “Optimization of NSLS-II Blade X-ray Beam Position Monitors: From Photoemission Type to Diamond Detector”, in *Proc. IBIC'13*, Oxford, UK, Sep. 2013, paper MOPC10, pp. 67-70.
- [8] M. Borland, "ELEGANT: A Flexible SDDS-Compliant Code for Accelerator Simulation," Advanced Photon Source LS-287, September 2000. doi:10.2172/761286